

A SIMPLIFIED MECHANICAL MODEL AND ITS DYNAMIC ANALYSIS ON AIRBORNE MINIATURE STABILIZATION PLATFORM

FENG LIU AND HUA WANG

School of Astronautics
Beihang University
No. 37, Xueyuan Rd., Haidian Dist., Beijing 100191, P. R. China
lfjssx@126.com

Received April 2016; accepted July 2016

ABSTRACT. *To reveal angular rate characteristics of inner-outer frame using coordinate transform, the model of two-axis and two-frame is constructed. Simulation results indicate that unknown disturbance torque and carrier coupling disturbance torques have large effect on the line of sight (LOS) of miniature stabilized platform. First, the unknown disturbance torque can be reduced by mechanical measures. Then, the carrier coupling disturbance torque need isolate carriers' disturbance by control system, which can be of significance for stable tracking under the driving of control instructions.*

Keywords: Two-axis and two-frame, Gyro-free, Disturbance torques, Pulses

1. **Introduction.** The stabilization platform [1, 2] is widely utilized in tracking, reconnaissance, and other military and civil fields, which is an indispensable component of maintaining LOS stable in the control system. Complete kinematics and dynamics models of the pitch/roll two-axis strapdown stabilization platform were built [3]. The equations of motion for the two axes yaw-pitch gimbal configuration were derived [4]. A complete gimbal kinematics and dynamics model of two-degree-of-freedom strapdown antenna platform was achieved via coordinate transformation based on configuration feature and stabilizing principle [5]. The motion equations of each were built with two-axis three-frame stabilized platform and dynamic analysis was made by ADAMS [6]. A mathematical model of the seeker was established to get the characteristics of pitch and azimuth of two-axis platform [7]. Previous researches only focus on kinematics and dynamics; however, the aforementioned discussions have not been found with such attempt on the motor and platform load transmission model. In this paper, the motor and platform load transmission model research about unknown disturbance and its torques pulse, coupling perturbation are comprehensively analysed. Therefore, this paper provides a supervisory for researching the disturbance and coupling characteristics. The remainder work is organized as follows. In Section 2, platform structure is introduced. In Section 3, the coordinate transformation is presented. In Section 4, the kinematical relationships are conducted. In Section 5, the inner-outer frame models are established. Simulation tests are generated in Section 6. The conclusions are summarized in Section 7.

2. **Platform Structure.** The structure of miniature stabilized platform about two-axis and two-frame [8] is shown in Figure 1.

3. **The Coordinate Transformation of Airborne Photoelectric Stabilized Platform.** The g , b , i and o stand for ground, body, inner frame, and outer frame coordinate system respectively in Figure 2(a). Suppose the unit vector under the inner frame coordinate system is $[1\ 0\ 0]^T$. The coordinate transform between inner frame and body is as

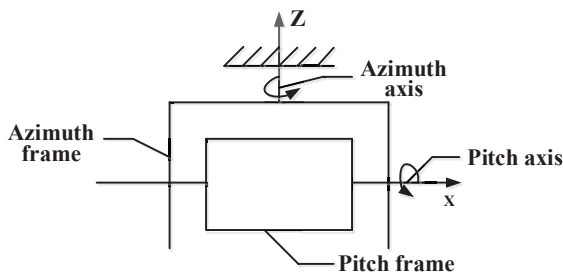


FIGURE 1. The photoelectric stabilized platform structure

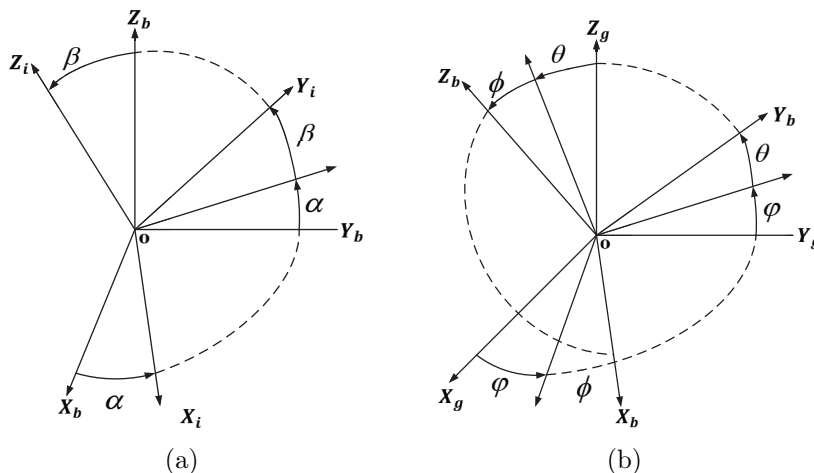


FIGURE 2. (a) Inner frame and body coordinate transform, (b) body and inertial coordinate transform

follows:

$$L_{b \leftarrow i} = \begin{pmatrix} \cos \alpha & \sin \alpha & 0 \\ -\cos \beta \cdot \sin \alpha & \cos \alpha \cdot \cos \beta & \sin \beta \\ \sin \alpha \cdot \sin \beta & -\cos \alpha \cdot \sin \beta & \cos \beta \end{pmatrix} \quad (1)$$

where α is the visual axis azimuth angular, and β is the LOS elevation angular.

Assume that the LOS axis is not deflection comparing with the body axis in initial time. The body coordinate system and inertial coordinate system's transformation is presented when the attitude changes in Figure 2(b). This transformation relationship is:

$$\begin{aligned} L_{b \rightarrow g} &= L_y(\phi) \cdot L_x(\theta) \cdot L_z(\varphi) \\ &= \begin{pmatrix} \cos \phi & 0 & -\sin \phi \\ 0 & 1 & 0 \\ \sin \phi & 0 & \cos \phi \end{pmatrix} \cdot \begin{pmatrix} 1 & 0 & 0 \\ 0 & \cos \theta & \sin \theta \\ 0 & -\sin \theta & \cos \theta \end{pmatrix} \cdot \begin{pmatrix} \cos \varphi & \sin \varphi & 0 \\ -\sin \varphi & \cos \varphi & 0 \\ 0 & 0 & 1 \end{pmatrix} \end{aligned} \quad (2)$$

where φ stands for the azimuth angle, θ represents the pitch angle, and ϕ is the roll angle.

4. The Kinematical Relationships of Photoelectric Platform.

4.1. **The framework angular velocity of the photoelectric platform.** According to the definition of the transformation between the outer frame and body coordinate system, the equation is as follows:

$$\begin{aligned} \omega_{go}^o(t) &= L_{o \leftarrow b}(t) \cdot \omega_{gb}^b(t) + \dot{\alpha}(t) \\ &= \begin{pmatrix} \cos \alpha & \sin \alpha & 0 \\ -\sin \alpha & \cos \alpha & 0 \\ 0 & 0 & 1 \end{pmatrix} \cdot \begin{pmatrix} \omega_{gb}^{bx} \\ \omega_{gb}^{by} \\ \omega_{gb}^{bz} \end{pmatrix} + \begin{pmatrix} 0 \\ 0 \\ \dot{\alpha} \end{pmatrix} \end{aligned} \quad (3)$$

The transformation matrix of the outer frame and body coordinate system is $L_{o\leftarrow b}$, the projection of ground to body coordinate system's transformation under body coordinate system is $\omega_{gb}^b(t)$, the projection of ground to outer frame coordinate system's transformation under the outer frame coordinate system is $\omega_{go}^o(t)$, and angular acceleration vector is $\dot{\alpha}(t) = [0 \ 0 \ \dot{\alpha}]^T$ when the outer frame is stable.

Similarly, the components of inner frame angular velocity is

$$\begin{aligned} \omega_{gi}^i(t) &= L_{i\leftarrow o}(t) \cdot \omega_{go}^o(t) + \dot{\beta}(t) \\ &= \begin{pmatrix} 1 & 0 & 0 \\ 0 & \cos \beta & \sin \beta \\ 0 & -\sin \beta & \cos \beta \end{pmatrix} \cdot \begin{pmatrix} \omega_{gb}^{bx} \cdot \cos \alpha + \omega_{gb}^{by} \cdot \sin \alpha \\ -\omega_{gb}^{bx} \cdot \sin \alpha + \omega_{gb}^{by} \cdot \cos \alpha \\ \omega_{gb}^{bz} + \dot{\alpha} \end{pmatrix} + \begin{pmatrix} \dot{\beta} \\ 0 \\ 0 \end{pmatrix} \end{aligned} \quad (4)$$

The coordinate transformation matrix of inner to outer frame is $L_{i\leftarrow o}(t)$, and the angular velocity vector of inner frame is $\omega_{gi}^i(t)$, $\dot{\beta}(t) = [\dot{\beta} \ 0 \ 0]^T$, so the projection of ground to body coordinate system's transformation under the body coordinate system is $\omega_{gb}^b(t)$.

4.2. Optoelectronic platform frame angular acceleration. The differential transformation of Equation (3) is the angular acceleration, and the expression is as follows:

$$\dot{\omega}_{go}^o(t) = L_{o\leftarrow b}(t) \cdot \dot{\omega}_{gb}^b(t) + \dot{L}_{o\leftarrow b}(t) \cdot \omega_{gb}^b(t) \cdot \dot{\alpha} + \ddot{\alpha}(t) \quad (5)$$

The angular velocity vector is $\dot{\omega}_{gb}^b(t) = [\dot{\omega}_{gb}^{bx}, \dot{\omega}_{gb}^{by}, \dot{\omega}_{gb}^{bz}]^T$, angular acceleration vector is $\ddot{\alpha}(t) = [0 \ 0 \ \ddot{\alpha}]^T$, and the angular velocity is $\dot{L}_{o\leftarrow b}(t)$ when the outer frame is stable.

Similarly, $\dot{\beta}(t) = [\dot{\beta} \ 0 \ 0]^T$. The angular acceleration vector of inner frame is:

$$\begin{aligned} \dot{\omega}_{gi}^i(t) &= \ddot{\beta}(t) + L_{i\leftarrow o}(t) \cdot \dot{\alpha}(t) + \dot{L}_{i\leftarrow o}(t) \cdot \dot{\alpha}(t) \cdot \dot{\beta} + C_o^i(t) \cdot \dot{L}_{o\leftarrow b}(t) \cdot \dot{\omega}_{gb}^b(t) \\ &+ \left[L_{i\leftarrow o}(t) \cdot \dot{L}_{o\leftarrow b}(t) \cdot \dot{\alpha} + \dot{L}_{i\leftarrow o}(t) \cdot L_{o\leftarrow b}(t) \cdot \dot{\beta} \right] \cdot \omega_{gb}^b(t) \end{aligned} \quad (6)$$

5. The Frame Model.

5.1. The inner frame model. Based on the Euler equation of fixed point motion of rotation rigid body, the kinetic model of the inner frame is:

$$\sum M_i = J_i \cdot \dot{\omega}_i + \omega_i \cdot J_i \cdot \omega_i = M_{el} - M_{fi} - M_{CRi} - k_{fi} \cdot \dot{\beta} - k_{CRi} \cdot \beta = M_{el} - M_{di} \quad (7)$$

where $\sum M_i$ represents total moment vector of inner framework. Let $M_{el} - M_{di} - M_{imbix} = J_{ix} \cdot \dot{\omega}_{ix}$, where $M_{imbix} = (J_{iz} - J_{iy}) \cdot \omega_{iy} \cdot \omega_{iz}$ denotes followed by nonlinear disturbance torque vector projection caused by the inner frame mass unbalance under three components of the coordinate system of inner frame. J stands for the moment of inertia matrix; ω is the angular velocity vector. Assuming the moment of inertia denotes distributed in the principal axis of inertia, then moment of inertia matrix stands for diagonal matrix, so $J_i = \text{diag}(J_{i/x}, J_{i/oy}, J_{i/z})$. $M_{fi/o}$ is the component coupling torque between frame and others' frame under the inner coordinate system; $M_{CRi/o}$ are the cable flexible nonlinear friction torque of the inner frame, outer frame; $k_{fi/o}$ are linear friction torque coefficient of the inner frame, outer frame; $k_{CRi/o}$ are cable flexible interference torque coefficient of the inner frame, outer frame; $M_{di/o}$ are the unknown disturbance torque of the inner frame, outer frame. There is only rotational freedom degree in the axis direction of inner frame, and the second component of Equation (7) is only effective. So the dynamics model of inner frame under inner frame axis is:

$$M_{el} - M_{imbix} - M_{di} = J_{ix} \cdot \dot{\omega}_{ix} \quad (8)$$

5.2. **The outer frame model.** The basic dynamic formula of outer frame is:

$$\begin{aligned} \sum M_o &= J_o \cdot \dot{\omega}_o + \omega_o \cdot J_o \cdot \omega_o + \left[\sum M_i \right]_o \\ &= M_{ro} - M_{fo} - M_{CRo} - k_{fo} \cdot \dot{\alpha} - k_{CRo} \cdot \alpha \end{aligned} \tag{9}$$

$\sum M_o$ is total torque vector of outer frame. Let $M_{do} = M_{fo} + M_{CRo} + k_{fo} \cdot \dot{\alpha} + k_{CRo} \cdot \alpha$. Do the coordinate transformation, so $M_{ro} - M_{imboz} - M_{do} = J_{oz} \cdot \dot{\omega}_{oz} - J_{iy} \cdot \dot{\omega}_{iy} \cdot \sin \beta$. M_{el} , M_{ro} are the motor driving torque of inner frame, outer frame. The transfer function is obtained utilizing the Laplace transformation.

$$M_{ro} - M_{imboz} - M_{do} = J_{oz} \cdot \dot{\omega}_{oz} - J_{iy} \cdot \dot{\omega}_{iy} \cdot \sin \beta \tag{10}$$

M_{imbox} and M_{imboz} are followed by nonlinear disturbance torque vector projection caused by the inner frame mass unbalance under three components of the coordinate system of outer frame, substitution and simplification, so

$$\left\{ \begin{aligned} \omega_{ix} &= \frac{k_{Ti} \cdot u_{ai}}{J_i \cdot R_{ai} \cdot s + k_{Ti} \cdot k_{ei}} + \frac{k_{Ti} \cdot k_{ei} \cdot \omega_{gb}^{bx} \cdot \cos \alpha}{J_i \cdot R_{ai} \cdot s + k_{Ti} \cdot k_{ei}} \\ &+ \frac{k_{Ti} \cdot k_{ei} \cdot \omega_{gb}^{by} \cdot \sin \alpha}{J_i \cdot R_{ai} \cdot s + k_{Ti} \cdot k_{ei}} - \frac{R_{ai} \cdot M_{di}}{J_i \cdot R_{ai} \cdot s + k_{Ti} \cdot k_{ei}} \\ \omega_{oz} &= \frac{k_{To} \cdot u_{ao} + k_{To} \cdot k_{eo} - R_{ao} \cdot M_{do}}{(J_o + J_i) \cdot R_{ao} \cdot s + k_{To} \cdot k_{eo}} \end{aligned} \right. \tag{11}$$

TABLE 1. The motor parameters of two-axis and two-frame stabilized platform

Parameter	1	2	3	4
J_i	2.566	2.566	2.566	2.566
J_o	1.676	1.676	1.676	1.676
R_{ai}	10.48	2.6	12.6	6.0
K_{ao}	6.3	7.7	1.4	5.4
R_{Ti}	10.49	0.01	0.028	0.004
R_{To}	0.028	0.065	0.045	0.079
R_{ei}	0.0008	0.002	0.003	0.0012
R_{eo}	0.004	0.008	0.004	0.01

6. **Simulation Tests.** The four types of motor parameters are obtained based on PROE to investigate the performance of LOS stable in Table 1, and the equations are solved according to the fourth order Runge-Kutta method when the step is 0.001s.

- Open loop unit step response

The effect of optical axis angular velocity is shown in Figure 3 when the input of unit step voltage signal in the framework of motor is taken into account.

The open-loop regulation time of M_1 , M_2 , N_2 model system is relatively short in Figure 3(a) and Figure 3(b), so it is necessary to improve the system response speed.

- Unit step unknown disturbance torque

The response under the unit step unknown disturbance torque is obtained when the unknown disturbance torque is 0.01 rad amplitude step signal in Figure 3(b). The optical axis angular velocity always presents negative growth until reaching steady state under the continuing role of disturbance torque, while the type of M_1 , M_2 motors needs short time when the optical axis angular velocity reaches steady state.

- Unknown disturbance torques pulse

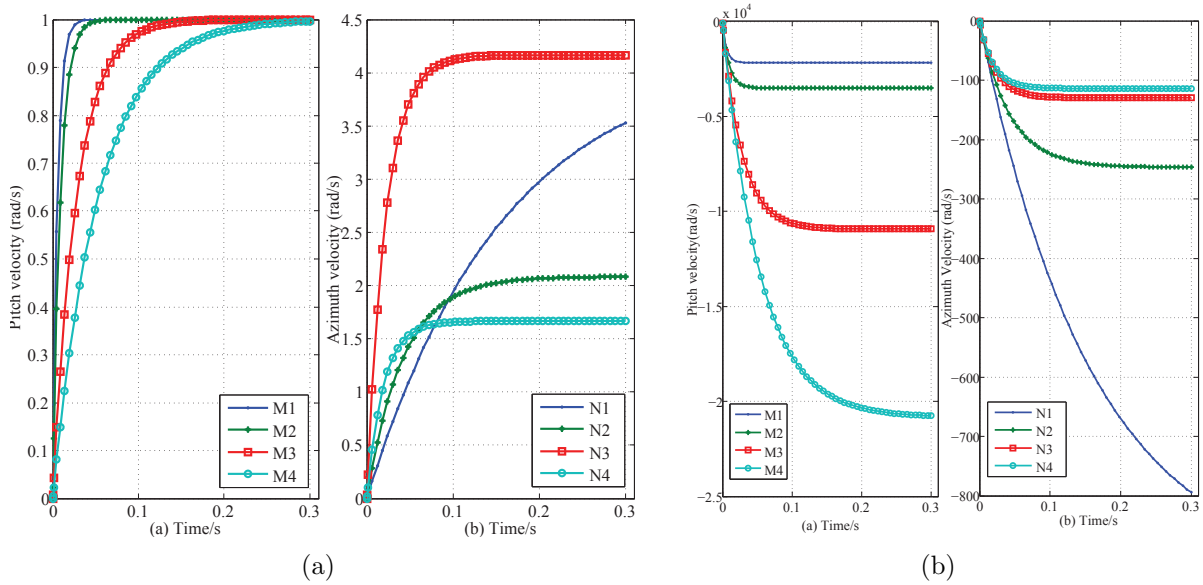


FIGURE 3. (a) Open loop unit step response, (b) the response under unit step unknown disturbance torque

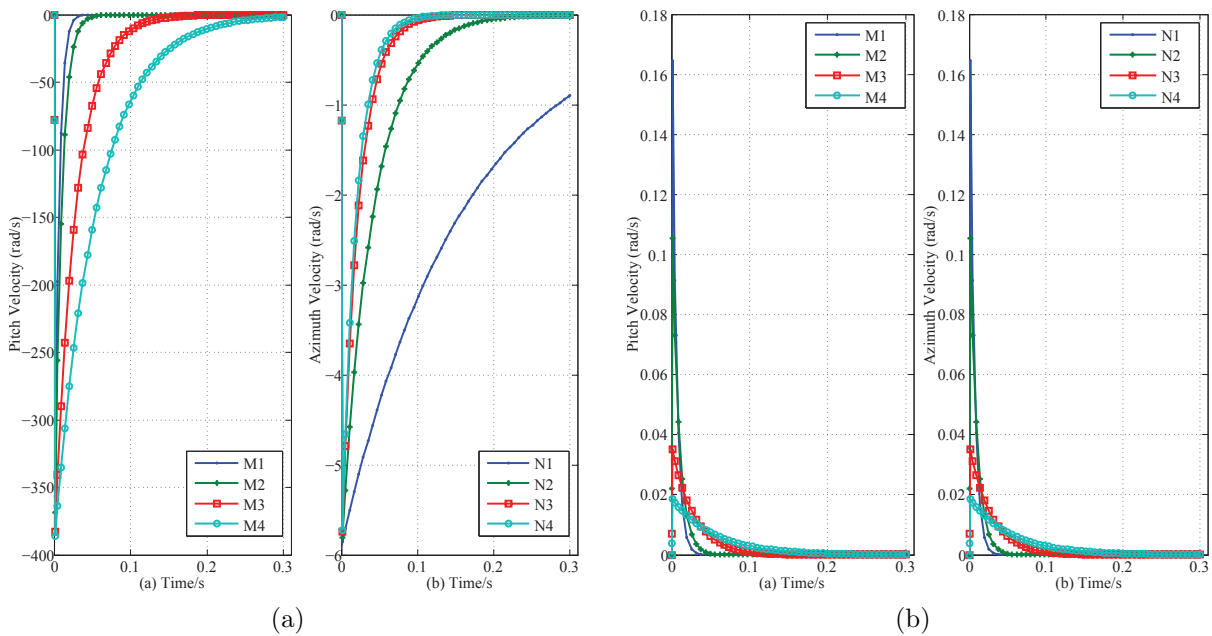


FIGURE 4. (a) Response under pulse unknown disturbance torque, (b) response under impulse vector coupling perturbation

The effects of optical axis angular velocity are obvious if torques pulse amplitude of unknown disturbance is 1N.m, width is 0.01s, and pulse signal is at 1s in Figure 4(a).

The optical axis angular velocity rapidly recovers to be zero position out of pulse disturbance from Figure 4(a). The trends that optical axis angle deviates from the zero position are decreased when angular velocity changes, and tends to be a constant, but optical axis angle could not be back to the balance position, so it can be compensated by the control system, and also can be avoided by mechanical measures.

- Coupling perturbation

The optical axis angular velocity is greatly influenced when pulse signal is 1s, carrier angular velocity is 1rad/s pulse amplitude, and width is 0.01s in Figure 4(b). Optical angle

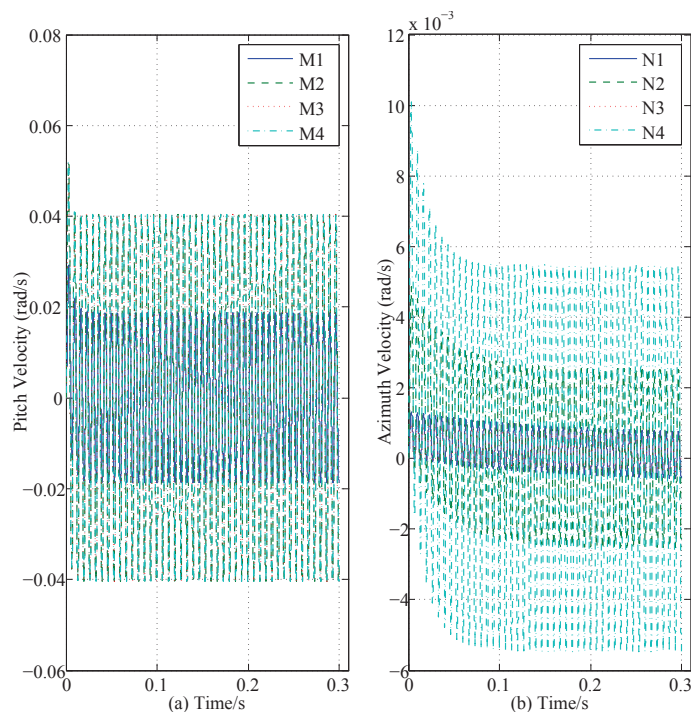


FIGURE 5. The response under the perturbed of sine carrier coupling

speed is fast disturbed and gradually recovers to be zero equilibrium position when the pulse disturbance is missing. The change will lead to quick deviation from zero balance position of the optical axis angle, eventually gradually reaching a new equilibrium position in Figure 4(b). The coupling disturbance influence on the optical axis angular velocity when carrier angular velocity is 1rad/s pulse amplitude, width is 0.01s and pulse signal is at 1s in Figure 5. The optical axis and carrier angular velocity have equal frequency continuous sinusoidal signals, and tend to be the equilibrium position but will not return to be the equilibrium position. Meanwhile, the optical axis angle deviates from the zero equilibrium position, and has equal frequency fluctuation.

7. Conclusions. A mathematical calculation method under gyro-free photoelectric stabilized platform is presented. The way of model construction is more superior comparison with locking one freedom degree based on three axes stabilized platform; moreover, the validity is well proved. Although unknown disturbance torque and carrier coupling disturbance torques have great effect on the LOS axis when two framework are under the conditions of different motor parameters. The control system can generally compensate the disturbance in engineering, and the location disturbance torque disturbance can be compensated by mechanics. The inner-outer frame stabilization loops of the control system and the stable controller design are further research directions to maintain LOS stable in inertial space in the future.

REFERENCES

- [1] J. M. Hilkert, Inertially stabilized platform technology concepts and principles, *IEEE Control Systems*, vol.28, no.1, pp.26-46, 2008.
- [2] P. J. Kennedy and R. L. Kennedy, Direct versus indirect line of sight (LOS) stabilization, *IEEE Trans. Control Systems Technology*, vol.11, no.1, pp.3-15, 2003.
- [3] D. Li, H. Zhang and Y. Zhao, Research on modeling and simulation for pitch/roll two-axis strap-down stabilization platform, *The 10th International Conference on Electronic Measurement and Instruments*, no.2, pp.42-46, 2011.
- [4] B. Ekstrand, Equations of motion for a two-axes gimbal system, *IEEE Trans. Aerospace and Electronic Systems*, vol.37, no.3, pp.1083-1091, 2001.

- [5] R. Zhao, S. Lü and X. Liu, Dynamics modeling and simulation analyzing for strapdown antenna stable platform, *Journal of Beijing University of Aeronautics and Astronautics*, vol.31, no.9, pp.953-957, 2005.
- [6] J. Wang et al., Dynamic analysis of optoelectronic stabilized platform with the structure of two axes and three frames, *Mechanical Design and Research*, vol.29, no.4, pp.33-47, 2013.
- [7] Y. Zhang, B. Liu and S. Yin, Strapdown optical seeker: Stabilization, tracking principle and system simulation, *Optics and Precision Engineering*, vol.16, no.10, pp.1942-1948, 2008.
- [8] Y. Zong, X. Jiang, X. Song et al., Design of a two axes stabilization platform for vehicle-borne opto-electronic imaging system, *2010 International Conference on Computational Problem-Solving*, pp.420-423, 2010.